

Dip and Strike Measured Systematically on Digitized Three-Dimensional Geological Maps

Jean Chorowicz

Département de Géotectonique, Université Paris 6, 4 place Jussieu, 77252 Paris, France

Jean-Yves Bréard

Institut Géographique National, 2 avenue Pasteur, 94160 St Mandé, France

Richard Guillaude, Claude-Roger Morasse, Didier Prudon, and Jean-Paul Rudant

Département de Géotectonique, Université Paris 6, 4 place Jussieu, 77252 Paris, France

ABSTRACT: A method of computing dips and strikes of geological contacts from a coregistered digital terrain model (DTM) and geological map data is developed and assessed. Examination of perspective views of the three-dimensional geological map were used to assess registration quality. The dips and strikes were systematically computed on an entire map at all the geological contact/thalweg crossing points using a three-point method. On the whole, the computed values are close to the ground truth, but they are generally steeper. Quality of map digitization and superimposition have then to be improved.

INTRODUCTION

THE MEASUREMENT OF DIPS AND STRIKES of features such as lithological surfaces, foliation, or faults is a necessary part of geological mapping and provides essential data to extrapolate surficial observations at depth. The number of measurements made in the field by the geologist using a compass-clinometer is limited because he cannot go everywhere. Geological contacts are usually plotted on the topographic base map, i.e., in a three-dimensional space. It is useful to determine systematically dips and strikes from digitized data and provide automatically a great number of measurements, opening the way to statistical analysis. It will be particularly helpful on a geologic interpretation of satellite data coregistered on a digital terrain model (DTM) compiled from stereoscopic SPOT data in the case where there are no available field measurements.

A DTM is now relatively easy to generate from stereoscopic data (Ungar *et al.*, 1983; Konecny *et al.*, 1987; Maître and Bardinnet, 1988; Renouard, 1988) in every part of the world, and it is worthwhile developing geologic applications. The computations of dips and strikes presented in this paper have been made on a DTM generated by digitizing contour lines. All the computations are applicable to any DTM.

The aim of this work is to develop an automatic method for the systematic measurement of dips and strikes of geological contacts that are superimposed on the DTM. Measurement is made at every crossing points with thalwegs. Several steps are necessary: digitization of the data, superimposition, computation of dips and strikes, and evaluation of the results. This work represents another, independently developed application of procedures first reported by Adam de Villiers and Leymarie (1984), Adam de Villiers (1985), Lang *et al.* (1987), and McGuffie *et al.* (1989).

This research has been carried out in the Sainte Victoire test-zone, in southeastern France (Figure 1) where we have recently completed a new 1:50,000-scale geological map (Chorowicz and Ruiz, 1985). Our technique was developed on a Domain network of Apollo computers, using Eagis software.

DIGITIZATION OF THE DATA

Digitization of the 1:50,000-scale geological map was carried out using an opto-electronic scanner method. The geological contacts were redrawn, photographically reduced, and digitized by scanner, resulting in an image whose pixel values range between 0 and 255. The file comprises 2,000 lines and 4,000

columns; each pixel represents a 5- by 5-m surface on the ground, which is consistent with the original map scale.

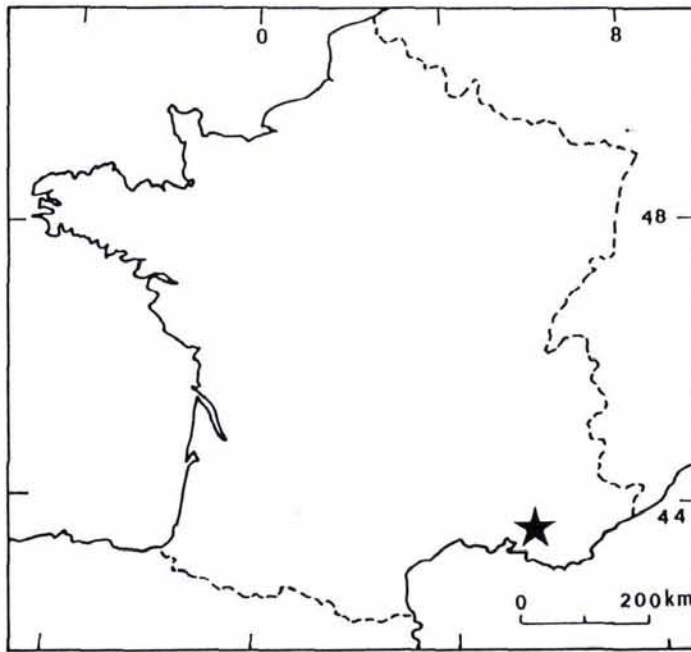
Because resulting map shows geological contacts only, it was necessary to color areas between contacts. The image was first transformed into a binary image and various oriented or unoriented dilatations and erosions were applied in order to obtain continuous contacts. Skeletonization processes gave thin regular lines. Colors corresponding to the stratigraphy were chosen from color tables and displayed on the screen using the accepted conventions in geology. Every surface on the map was then colored accordingly (Plate 1A).

The DTM was generated by digitizing 20-m contour lines obtained from 1:60,000-scale stereoscopic aerial photographs utilizing analog photogrammetry. The contour lines were extrapolated in 50-m steps using the "elastic grid" method (de Masson D'Autume, 1978). This value, being inconsistent with the 5- by 5-m pixel size of the digitized geological map, the DTM was afterwards resampled during the superimposition process. The elevations, ranging in the test area from 245 to 1011 m, are coded in 8 bits, resulting in a sampling interval of about 3 m in elevation.

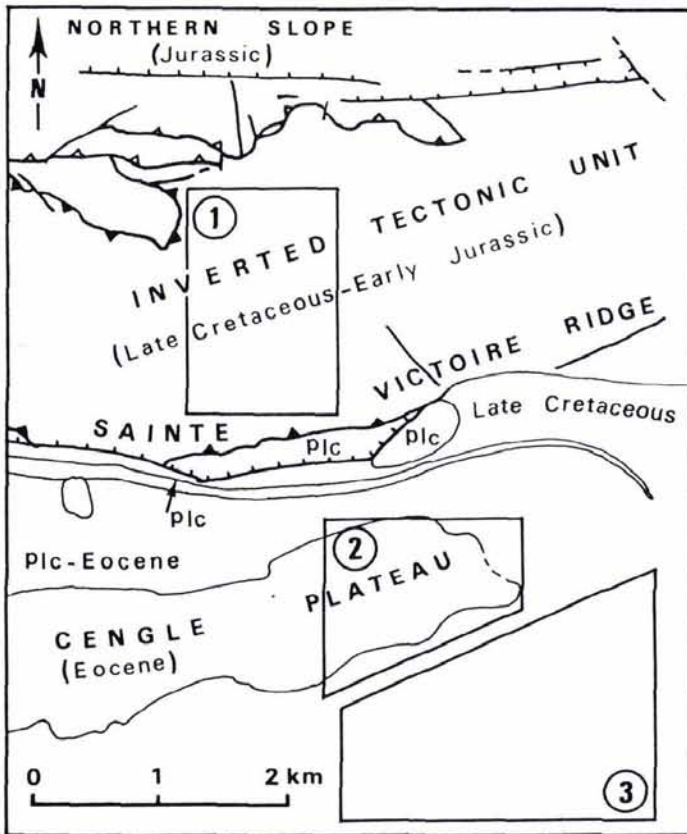
SUPERIMPOSITION DTM/GEOLOGICAL MAP

Because the digital geological map and the DTM do not have consistent sampling, projection, orientation, and covered ground surface, it was necessary to relate them to the same geometry. The choice of tie points on the geological map is relatively easy. However, several types of images had to be formed from the DTM, including contour lines, elevations displayed at grey levels, and shaded relief images. The latter images efficiently highlight subtle topographic features when computed with different low-angle azimuths. Most of the tie points are located on the DTM with an error interval of one pixel, i.e., 50 m. We used 36 pairs of tie points. The DTM map was then transformed to fit the geological map because it is easier to resample large pixels. We used a second-order polynomial transformation that takes into account not only rotations and translations but also deformations of greater magnitude. Resampling was accomplished using a bicubic process.

Reliability in matching the digital geological map to the resampled DTM may be assessed by observation of perspective views (e.g., Plate 1A). These expose the color geological map superimposed onto the shaded relief DTM and give a detailed three-dimensional view of the test area. The best views are ob-



(A)



(B)

FIG. 1. (A) Location of the Sainte Victoire test area, in Provence (southeastern France). (B) Schematic structural pattern of the Sainte Victoire test area. (1), (2), and (3): location of the zones used to assess the validity of the computed dips and strikes. Line with triangles: thrust lines. Line with teeth: normal fault (teeth away from the uplifted compartment). Plc: Paleocene.

tained when the illumination and observation azimuths are at right angles. When the geological and geomorphological features seem visually well correlated, the result of the matching process may be considered as correct. In this case, the geological map is easier to interpret than the usual printed map sheets because it is possible to change the points of view in azimuth and in elevation.

On Plate 1A, it can be seen that the crest line of the Sainte Victoire ridge is formed by a thick lithologic unit consisting of overturned Late Jurassic reef limestones, colored in yellow, which in the east lie upon Early Cretaceous marls (green). The Late Jurassic reef limestones (Figure 1B) are thrust southwards over the autochthonous Cengle Plateau consisting of sub-horizontal continental units (orange, light yellow, brown, and white colors) which are conformably lying on Late Cretaceous continental rocks (blue-green). The main thrust is separated from the autochthon by normal faults in the western segment but it passes alongstrike eastwards into a stratigraphic contact. The northern slope of the ridge consists of a normal succession of Jurassic marine rocks ranging from the Liassic (light green) to the Dogger (red) and the Malm (dark and light blue) which is thrust over the overturned Late Jurassic reef unit.

COMPUTATION OF DIPS AND STRIKES

The geological contacts are now in three-dimensional space with each pixel representing a 5- by 5-m square on the ground. Elevation value spacing is 3 m (see supra). Assuming locally planar contact, three different points belonging to the same contact segment define a plane which represents the local approximation of the surface separating two lithologic units. The following dip and strike characteristics (Figure 2) are computed from the coordinates of this plane: the azimuth (a) of the intersection of this plane with a horizontal plane is the strike, the azimuth of the main downgrading slope line (c) gives the dip direction, and the angle (d) between this main downgrading slope line and a horizontal plane is the dip.

We chose to seek the intersections of the geological contacts with thalwegs to find three unaligned points for calculating dip. Flat irons or any three points at the contact would do equally as well, but we find points not associated with thalwegs less precise for giving reliable results by systematic automatic computing and they are not taken into account in this paper.

Our method for automated dip determination involves three steps: (1) extraction of the thalwegs from the DTM; (2) location of the crossing points between thalwegs and geological contacts and positioning of three-point groups; and (3) computation of the dip and strike characteristics for each three-point set, assuming coplanarity.

EXTRACTION OF THALWEGS FROM THE DTM

Several methods for the extraction of thalwegs from DTM are described in the literature (O'Callaghan and Mark, 1974; Collins, 1975; Chorowicz, 1984; Papo and Gelbman, 1984; Douglas, 1986; Martz and De Jong, 1988; Morris and Meerdegen, 1988; Riazanoff *et al.*, 1988); here we used the simple "local minima" method.

Analysis of the DTM was made automatically along profiles following the lines and the columns, searching for flat or sharp valleys (Figure 3A). Five elementary topographic features, defined as "types" on Figure 3B, may exist along the profiles. Type 3 or a succession of types 1 and 2, with or without type 4 in between, satisfy our requirements. To find precise crossing points, only the narrow thalwegs can be used: we have deleted all the flat valleys having more than six pixels in width.

Extraction of the thalwegs was successful, as can be appreciated from Plate 1B, which represents skeletonized thalwegs superimposed onto the shadowed DTM. All the thalwegs are selected except for those located in the nearly flat areas (i.e.,

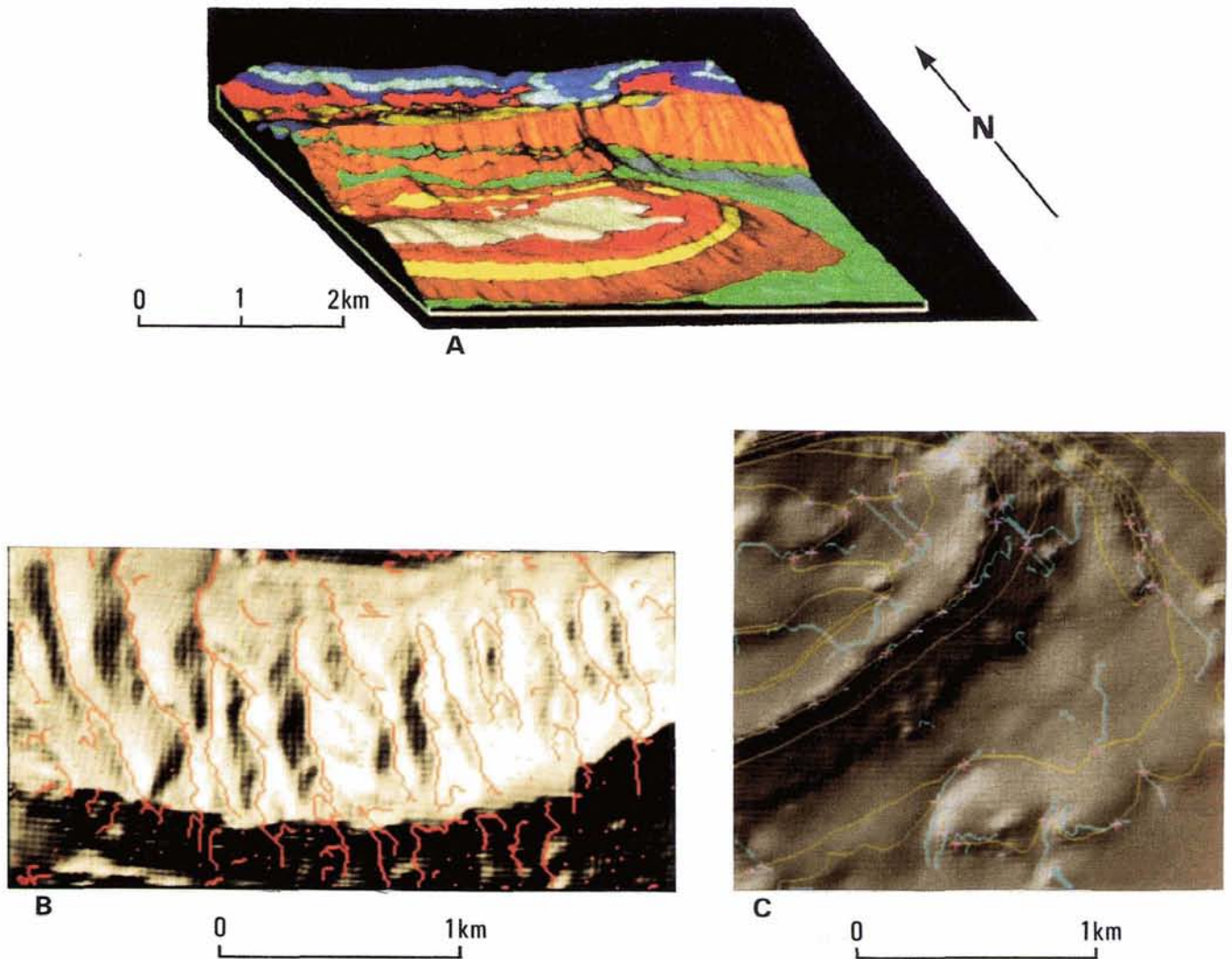


PLATE 1. (A) Perspective view of the digital geological map of the Sainte Victoire ridge, superimposed on the shaded relief DTM. The area covered by the map corresponds to Figure 1B. See explanation of the colors in text. (B) Superimposition of the skeletonized thalwegs onto the shaded relief DTM. (C) Screen image permitting access to the dip and strike files. When pointing the cursor on a red cross, the dip and strike computed at this location is automatically displayed. Yellow lines: geologic contacts; blue: thalwegs.

valleys more than six pixels in width). Starting from the shaded relief DTM, it is possible to improve the result in flat areas by manually drawing thalwegs with the cursor.

POSITIONING OF THE GROUPS OF THREE POINTS

The lowest of the three points (A) to be positioned is located right at the contact-thalweg intersection. B and C will be located in a 15- by 15-pixel window centered on A (Figure 4).

It is first necessary to determine the thalweg trend with respect to the directions of the lines and columns and the oblique directions of the window grid. These directions are successively considered at each contact-thalweg crossing intersection. For each direction, the pixels belonging to the thalweg are counted: the direction of the thalweg fits with the direction having the highest number of thalweg-pixels counted.

To determine the position of points B and C (Figure 4), it would be possible to follow the contact on each side of point A, but the lines are not always thin and they may sometimes be discontinuous. In addition, it is important to take several B and C points along the contact to form several three-point groups in order to minimize the effects of aberrant A points (Figure 5).

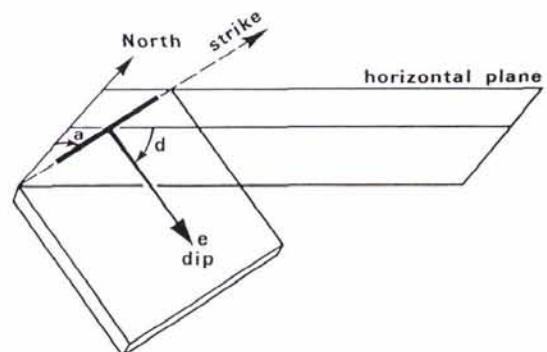


FIG. 2. Scheme defining the characteristics of the dip and strike taken into account in the computations: strike (in azimuth, a), sense of dip (e), and amount of dip (d).

We chose to define seven zones on each side of the thalweg (Figure 6), select the zones one by one, and find the points

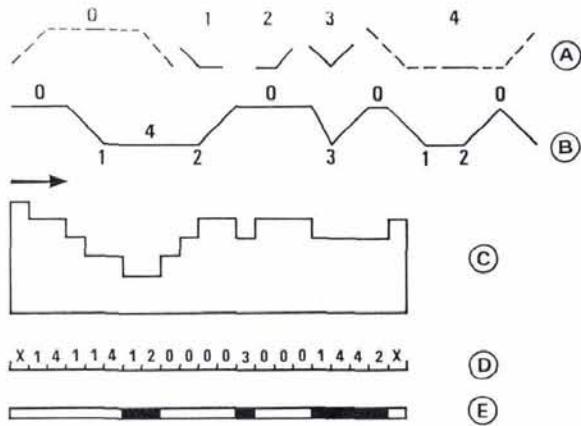


FIG. 3. Principle of the extraction of the thalwegs from the DTM. (A) elementary features, read from left to right; element 0: part of a summit or of an upgrading step; element 1: downgrading step; element 2: upgrading step; element 3: narrow thalweg (1 pixel); element 4: part of a large thalweg or of a downgrading step. (B) succession of schematic elementary features. (C), (D), and (E): example of detection of thalwegs from consideration of the elementary features along profile B. (C) profile across the DTM; (D) succession of elements along the profile; (E) thalwegs (in black).

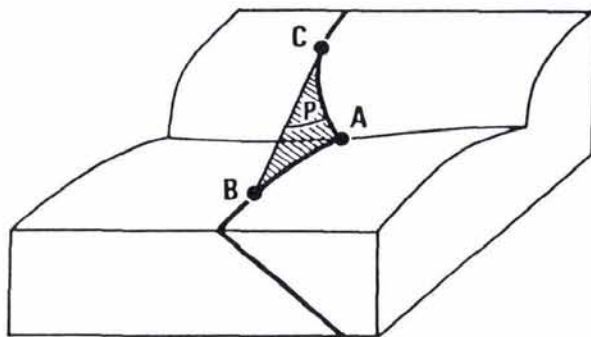


FIG. 4. Definition of the three points used for dip and strike computation.

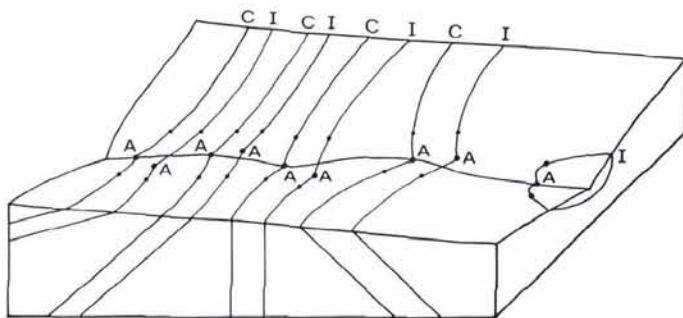


FIG. 5. Positioning of a point (A) used for dip and strike computation, at the crossing point between a geological contact and a thalweg. C: correct positioning; I: incorrect positioning.

belonging to geological contact included in each zone. There is a maximum of seven points B and 7 points C possible. In each half-zone having several contact points, we selected the center of the cluster of contact points. If the number of contact points is more than three, the dispersion is too important and the point B or C is rejected. When no point B or C is found, the point A

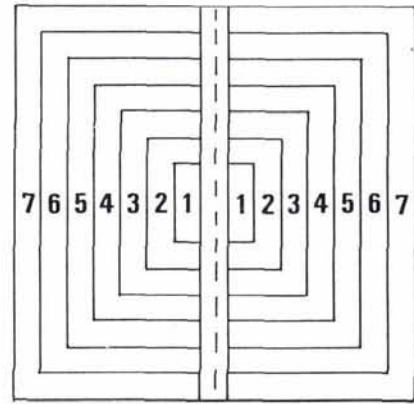


FIG. 6. Principle of determination of points B and C on each sides of a thalweg which is represented by dashed lines (comments in the text).

is rejected; otherwise, the three-point set formed by point A and on both sides by points B and C located in the same labeled area (from 1 to 7) is selected.

COMPUTATION

Each set of points A, B, and C (Figure 4) defines a plane (P). Dips and strikes were determined using three-point problem solutions (Compton, 1962; Ragan, 1973).

The computation is made at each point A for all the possible planes ABC. The file of the results includes, for each point A,

- the image coordinates of point A;
- a character string presenting clearly the result, e.g., 27 SE 55 (azimuth, direction of dip, amount of dip);
- the mean and variance of the amount of dip;
- the mean and variance of the strike;
- the number of ABC point sets used;
- the senses of dip for each group; and
- the strikes for each group.

This file can be used to consult the statistics concerning each dip and strike and eventually eliminate aberrations. The screen displays in superimposition the shaded relief DTM, thalwegs, geological contacts, and small crosses showing the emplacements of points A where dip and strike were computed (Plate 1C). Placing the cursor on a cross, access is gained to the file of results concerning this point. It is then possible to delete an aberrant measurement or to enter a measurement of dip and strike made in the field.

VALIDITY OF THE COMPUTED DIPS AND STRIKES

To assess the validity of the computed dips and strikes, we have compared a part of the 167 measurements obtained in the test area with the 18 illustrated on our geological map and the previous 1:50,000-scale regular geological map and with estimates from the published cross-sections. Three differently configured typical zones of the test area have been selected (Figure 1B): northern back-slope of the Sainte Victoire ridge (zone 1), Cengle Plateau (zone 2), and flat country southeast of the Cengle Plateau (zone 3). These zones expose stratigraphic contacts that are supposedly parallel to the layers, and their dips and strikes (computed) may be compared with field measurements. The dips and strikes of these zones vary from east to west. Computed results are compared with the nearest field measurement in Table 1.

Zone 1 exposes steep slopes, deep thalwegs, well defined flat-irons, and steep dips. The computed and the field values are more or less close. Zone 2 is a plateau area, while the flat-irons

TABLE 1. COMPARISON BETWEEN THE COMPUTED DIPS AND STRIKES AND THE FIELD MEASUREMENTS OR ESTIMATIONS.

Computed dip and strike		Nearest field dip and strike	
Azimuth	Dip	Azimuth	Dip
Zone 1			
94	N 83		
97	N 81	E-W	N 59
60	NW 61	E-W	N 63
97	N 78	E-W	N 87
88	N 74		
80	NW 84		
77	NW 22	E-W	N 47
71	NW 47	E-W	N 41
90	N 90	E-W	N 58
94	N 69		
105	N 65	E-W	N 59
140	NE 63	E-W	N 43
155	NE 59	E-W	N 42
103	N 65	E-W	N 56
123	NE 81	E-W	N 53
98	N 69	E-W	N 64
82	N 64	E-W	N 60
90	N 67	E-W	N 60
94	N 58	E-W	N 58
69	NW 60	E-W	N 60 N 74
72	NW 73	E-W	N 58 N 66
58	NW 69	E-W	N 64 N 54
100	N 59	E-W	N 60 N 76
91	N 83		
81	N 73		
61	NW 76		
Zone 2			
171	ENE 59		
172	SW 66	NE	NW 15
172	SW 59		
146	NE 29		
135	SW 23	E-W	N 15
Zone 3			
174	W 12	ENE	NNW 15
179	W 34	ENE	NNW 13
119	SW 10	NE	NW 12
162	WSW 15	NE	NW 11
165	WSW 3	NE	NW 10
171	WSW 16	NE	NW 10

are more open and less evident. Zone 3 is also a flat area. Zones 2 and 3 are both characterized by flat dips. The computed dips are then spread over a large interval of values. The strike of the subhorizontal beds is imprecise because computation of the strike of a near horizontal plane is imprecise. The automatic computation tends to give steeper dips than the field measurements.

Incorrect dip and strike values may arise from a poor matching between the digital geological map and the DTM. In this case, the crossing point A may not be exactly located at the apex of the V which is shaped on the map by the geological contact crossing the thalweg (Figure 5). The use of a DTM generated from a stereopair of panchromatic SPOT scenes with a 10-by-10-m pixel size might reduce this imperfection insofar as the geological map would be drawn directly onto the SPOT image displayed on the screen in the same geometry as the DTM. Another type of error is related to a local rapid variation of the dips and strikes due, for instance, to a small fold (Figure 5).

To eliminate these problems, it is possible to manually re-shape more precise contacts across the thalwegs with the cursor. Normally, the geologist has to take care that the apex of the V is right at the intersection with the thalweg and that the shape of the V is not smoothed due to rapid drawing, resulting

in steeper dips than in reality. The smoothing of the V may also result from the erosion-dilatation-skeletonization processes.

Our method could be improved, for instance, in having the possibility to adapt the dimensions of the grid defining the points B and C on each side of the point A with regard to the topographic characteristics of the region concerned. In flat areas, a larger grid would be more efficient. In an area with sharp topographic features, a large grid would, however, include in the computation pixels belonging to more than one thalweg, resulting in an incorrect measurement. The size of the grid we have chosen here seems to fit with the configuration of the Sainte Victoire area. A different size may be necessary in other areas.

If we eliminate measurements having too large a standard deviation, indicating a local problem (e.g., a small fold), our dip and strike measurements would still be on the whole close enough to ground observations to be of value in structural analysis. They are much more numerous than those plotted on the maps, rapidly and systematically computed at each thalweg/contact intersection, and they provide a consistent geological information which will be used for the automatic drawing of geologic cross sections or for statistical analysis.

CONCLUSION

On coregistered geologic contacts and DTM data, our method systematically computes dips and strikes of geological contacts at every crossing point with thalwegs. It then provides very rapidly a great number of measurements.

Differences occur between automatically computed dips and strikes and field measurements, the computed dip values being generally exaggerated, more particularly in flat areas. The actual accuracy of the result is dependent upon the quality of digitization and superimposition of the data.

ACKNOWLEDGMENTS

The authors are indebted to H.R. Lang for beneficial review and suggestions. The manuscript has been also improved by constructive comments from two anonymous reviewers.

REFERENCES

- Adam de Villiers, D., 1985. *Utilisation géologique du traitement d'images appliqué aux modèles numériques de terrain. Exemples du Nord Limousin et du plateau de Millevaches*. Thèse, Ecole Nationale Supérieure des Mines de Paris, 150 p.
- Adam de Villiers, C., and P. Laymarie, 1984. Cartographie automatique des situations topographiques en vue d'utilisations géologiques. *Computers in Earth Sciences for Natural Resources Characterization* (J.J. Royer, Editor), Nancy, pp. 333-350.
- Band, L. 1986. Topographic partition of watersheds with digital elevation models. *Water Resources Research* 22(1):15-24.
- Chorowicz, J., 1984. Importance of pattern recognition for geological remote sensing. *Remote Sensing for Geological Mapping* (P. Teleki and C. Weber, eds.), Documents BRGM no. 82, Publication IUGS, 18, pp. 29-40.
- Chorowicz, J., and R. Ruiz, 1984. La Sainte Victoire (Provence): observations et interprétations nouvelles. *Géologie de la France*, B.R.G.M., no.4, pp. 41-55.
- Collins, S. H., 1975. Terrain parameters directly from a digital terrain model. *Canadian Surveyor* 29(5):507-508.
- Compton, R. R., 1962. *Manual of Field Geology*. New York, John Wiley, 378 p.
- Douglas, D. H., 1986. Experiments to locate ridges and channels to create a new type of digital elevation model. *Cartographica* 23(4):29-61.
- Konecny, G., P. Lohmann, H. Engel, and E. Kruck, 1987. Evaluation of SPOT imagery on analytical photogrammetric instruments. *Photogrammetric Engineering & Remote Sensing* 53(9):1223-1230.
- Lang, H. R., S. L. Adams, J. E. Conel, B. A. McGuffie, E. D. Paylor,

- and R. E. Walker. 1987. Multispectral remote sensing as stratigraphic and structural tool, Wind River Basin and Big Horn Basin areas, Wyoming. *A.A.P.G. Bull.* 71(4):389-402.
- Maitre, H., and C. Bardinnet, 1988. Digital stereo relief construction of Tanzania (Karema region) using aerial imagery. *Image analysis, geological control and radiometric survey of Landsat-TM data in Tanzania*, (J. Lavreau and C. Bardinnet. eds.), Musée Royal de l'Afrique Centrale, Tervuren Belgique, Annales 96, pp. 131-138.
- Martz, W. L., and E. De Jong, 1988. CATCH: A FORTRAN program for measuring catchment area from Digital Elevation Models. *Computers and Geosciences* 14(5):627-640.
- Masson d'Autume (de), M. G., 1978. Construction du modèle numérique d'une surface par approximations successives. *Bull. Société Française de Photogrammétrie et Télédétection* 3/4:33-41.
- McGuffie, B. A., L. F. Johnson, R. E. Alley, and H. R. Lang, 1989. Computer-aided photogeologic mapping with image processing, graphics and CAD/CAM capabilities. *Geobyte*, pp. 8-14.
- Morris, D. G., and R. G. Meerdegen, 1988. Automatically derived catchment boundaries and channel networks and their hydrological applications. *Geomorphology* 2:134-141.
- O'Callaghan, J. F., and D. H. Mark, 1984. The extraction of drainage networks from digital elevation data. *Computer Vision, Graphics and Image Processing* 28:323-344.
- Papo, H. B., and E. Gelbman, 1984. Digital terrain models for slope and curvatures, *Photogrammetric Engineering & Remote Sensing* 35:695-701.
- Ragan, D. M., 1973. *Structural Geology: An Introduction to Geometrical Techniques*. New York, John Wiley, 208 p.
- Renouard, L., 1988. Création automatique de MNT à partir de couples d'images SPOT. *SPOT 1, Utilisation des images, Bilans, Résultats*, Paris, pp. 1347-1356.
- Ryazanoff, S., B. Cervelle, and J. Chorowicz, 1988. Ridges and valleys line extraction from digital image. *Int. J. of Remote Sensing* 9(6):1175-1183.
- Ungar, S. G., R. Irish, C. J. Merry, A. H. Strahler, H. L. McKim, B. Gauthier, G. Weill, and M. S. Miller, 1983. Extraction of topography from side-looking satellite systems; a case study with SPOT simulation data. *Proc. Int. Symp. Rem. Sens. Environm.* 17:535-550.

(Received 26 March 1990; revised and accepted 3 August 1990)

SPATIAL DATA 2000

CALL FOR CONFERENCE PAPERS

Spatial Data 2000 intends to be a platform for people from a wide range of disciplines who have an interest within the increasingly important area of spatial information. The main discussions at the conference will revolve around papers presented by invited speakers who will set the scene for particular topics. Individual contributions may be made to the discussion or through poster presentations.

Contributors wishing to present a poster paper on a subject relevant to the conference theme are invited to submit an abstract of not more than 250 words to the Conference Director by the 1st May 1991. Poster papers received will be reviewed and selections will be made by a panel of representatives from the three sponsoring societies. Individuals whose papers are selected will be notified by 1st June 1991.

The poster sessions have been scheduled to run sequentially with other activities and all papers will be published in the conference proceedings, available at Christ Church in September.

Please forward papers to the Conference Director : Professor Ian Dowman, Spatial Data 2000, Department of Photogrammetry and Surveying, University College London, Gower Street, London, WC1E 6BT, England. Telephone: 071-380-7226. Fax: 071-387-8057.

Christ Church, Oxford University, England, 17-20 September 1991

First jointly sponsored conference by The Photogrammetric Society, The Remote Sensing Society and The American Society for Photogrammetry and Remote Sensing

Notice - Change in Production Schedule

1991 Directory of the Mapping Sciences to be Published in June

The June issue will also be a special issue on GIS and Remote Sensing.

Contact our advertising department if you would like to advertise in the Directory or wish to change your advertising schedule.